ASAP: A Hybrid Computer Platform Using Machine Learning and Solar Imaging for Automated Prediction of Solar Flares

T. Colak[1] and R. Qahwaji [2]

[1] University of Bradford, Bradford, United Kingdom, t.colak@bradford.ac.uk

[2] University of Bradford, Bradford, United Kingdom, r.s.r.qahwaji@brad.ac.uk

Abstract

The importance of real-time processing of solar data especially for space weather applications is increasing continuously. In this paper, we present an automated hybrid computer platform for the short-term prediction of significant solar flares using SOHO/MDI images. This platform is called the Automated Solar Activity Prediction tool, or simply ASAP. This system integrates image processing and machine learning to deliver these predictions. A machine learning-based system is designed to analyze years of sunspot and flare data to create associations that can be represented using computer-based learning rules. An imaging-based real time system that provides automated detection, grouping and then classification of recent sunspots based on the McIntosh classification is also created and integrated within this system. The properties of the sunspot regions are extracted automatically by the imaging system and processed using the machine learning rules to generate the real-time predictions. Several performance measurement criteria are used and the results are provided in this paper. Also, Quadratic Score (QR) is used to compare the prediction results of ASAP with NOAA Space Weather Prediction Center (SWPC) between

1999 and 2002, and it is shown that ASAP generates more accurate predictions compared to SWPC.

1 Introduction

Space weather is defined by the U.S. National Space Weather Program (NSWP) as "conditions on the Sun and in the solar wind, magnetosphere, ionosphere, and thermosphere that can influence the performance and reliability of space-borne and ground-based technological systems and can endanger human life or health" (Koskinen et al., 2001). The importance of understanding space weather is increasing because extreme solar eruptions could affect our daily life activities. For example, there is a steadily increasing reliance on communications and power systems, both vulnerable to space weather.

The most dramatic solar activity events affecting the terrestrial environment are solar flares and Coronal Mass Ejections (CMEs) (Pick et al., 2001). Solar flares and CMEs are solar eruptions that can spew vast quantities of radiation and charged particles into space (Lenz, 2004). The ability to predict major solar storms can give companies sufficient lead time to implement preventive measures (Lenz, 2004). Satellite operators, space agencies, aviation industry, power generation and distribution industry, oil and gas industry and railways can benefit from an effective space weather prediction system

Solar activity is the driver of space weather. An efficient approach for the prediction of solar activities should use real-time, high-quality data and data processing techniques (Wang et al., 2003). We designed an automated space weather prediction service that combines solar physics with advanced image processing and machine learning techniques. Warning of eruptions can be initiated if appropriate instruments to observe the Sun, are combined with efficient data processing techniques. Predicting solar flares is important for space weather applications. These warnings could also provide indirect prediction for some energetic

particle events. This could provide useful lead time because some of these events can be seen at Earth within 10-15 minutes of the occurrence of the flare. Furthermore, if the prediction system generates low flaring probability with a high degree of confidence, one can argue that the probability for an energetic particle event is low. Such prediction could be useful for all those applications affected by energetic particles.

There are various research groups and organizations scattered around the world that are working on solar analysis and forecasting. These analyses and forecasts are typically subjective and depend mainly on the expert knowledge which may lead to occasional inconsistencies in performance. On the other hand, objective computerized analysis of solar images can provide automated processing and relatively consistent performance by using the large computational capabilities of modern computers to analyze and compare large amounts of recent and historical data. However, the real challenge today is to design high-performance and accurate computer-based systems.

To our knowledge, there has been no fully automated system that can provide real-time prediction of significant solar flares. The accuracies of the previous semi-automated systems that have been designed are generally lower compared to the performance provided by subjective analysis. For example, WOLF (Miller, 1988) is an expert system that has been created to analyze active regions and sunspots and then predict the probability of solar flare occurrence. WOLF has a knowledge base consisting of a set of “if-then” rules and an inference engine which applies these rules. Manual user interaction is required to provide a description for the observed active region and sunspots. WOLF would then determine the McIntosh classification for the associated sunspot and hence, the probability of the described group producing a flare of specified X-ray intensity.

THEO (McIntosh, 1990) is another expert system that is also based on the McIntosh classification system, but includes information on spot growth, rotation and shear, and inferred magnetic topology. ARM (Active Region Monitor) is an another solar flare forecasting system that has been developed to estimate the probability for a certain active region to produce C-, M-, or X-class flares . The percentage probabilities are based on the number of flares produced by regions classified by NOAA using the McIntosh classification scheme during cycle 22 (Gallagher et al., 2002). All these systems are not fully automated as they require user interaction to provide the properties and classifications of active regions as inputs and are not designed to extract data from solar images directly or automatically.

In this paper we introduce our fully automated pilot system called ASAP (Automated Solar Activity Prediction), which integrates image processing, machine learning and solar physics to provide automated prediction of solar flares based on the characteristics of sunspots. The prediction system is composed of two major stages: an image processing system and a machine learning system. The imaging system processes MDI continuum and magnetogram images in real-time to detect and classify sunspot groups and then determine their properties. The machine learning system is trained using historical sunspot and flare data. Association algorithms are designed to associate flares with the sunspot groups that caused them and to create training sets that are used to train the learning algorithms and produce computerized learning rules. We will demonstrate the reliability of this system by testing it on recent solar images and comparing the generated predictions with the actual solar flares reported in solar catalogues.

This paper is organized as follows: Section 2 describes the imaging system that is responsible for the automated grouping and classification of sunspots, Section 3 describes the machine learning system that is trained on historical sunspot and flare data. The integration,

performance and evaluation of the whole system are discussed in Section 4. The concluding remarks and suggestions for future work are presented in Section 5.

2 Sunspot Detection and Classification

A computer system that can automatically detect, group, and classify sunspots based on the McIntosh classification was presented in (Colak and Qahwaji, 2008). This system applies imaging techniques to SOHO/MDI continuum and magnetogram images to detect sunspot regions and extract their properties including their McIntosh classifications. In this work, this system for the first time is integrated with a machine learning-based system to provide real-time prediction for the possible occurrence of flares, as described in the next section.

2.1 SOHO MDI images

The MDI instrument on SOHO provides routine observations of the Sun in the white light continuum, in the vicinity of the Ni I 6767.8 Å photospheric absorption line. The instrument images the sun with a 1024x1024 CCD camera (Scherrer et al., 1995). MDI continuum images may be used as a white light equivalent for the purposes of sunspot observations. SOHO provides two to four MDI intensitygram images per day and twice as many magnetogram images with coverage which has been continuous since 1995.

MDI magnetogram images are used to measure the velocity and line-of-sight magnetic flux density in the Sun's photosphere. The magnetogram images show the magnetic flux density of the solar photosphere, with black and white areas indicating opposite magnetic polarities. The dark areas are regions of negative magnetic polarity (pointing toward the Sun) and the white regions have positive magnetic polarity (pointing outward). These images can be used for detecting active regions.

2.2 Summary of sunspot detection and classification algorithms

The detailed description, design, implementation and evaluation of this part of the system was presented in (Colak and Qahwaji, 2008). Our automated sunspot detection, grouping and classification algorithm consists of three main stages: pre-processing, sunspot detection and grouping, and sunspot classification. These stages can be summarized as follows:

Pre-processing of MDI images

Stage-1 processing: Applied to both continuum and magnetogram images.

- Detect the solar disk, determine its radius and centre, create a mask and remove any information or marks (i.e., date and direction) from the image using the mask.
- Calculate the Julian date and solar coordinates (The position angle, heliographic latitude, heliographic longitude) for the image using the equations in (Meeus, 1998).

Stage-2 processing: Applied only to magnetogram images.

- Map the magnetogram image from Heliocentric-Cartesian coordinates to Carrington Heliographic coordinates.
- Re-map the image to Heliocentric-Cartesian coordinates. Use centre, radius and solar coordinates of the continuum image as the new centre, radius and solar coordinates of the magnetogram image.

Sunspot grouping (Figure 1)

- Detect sunspot candidates from MDI continuum images using intensity thresholding.
- Detect active region candidates from MDI magnetogram images using morphological image processing algorithms like intensity filtering, dilation and erosion. More

information about the use of these algorithms for the detection of active regions can be found in (Colak and Qahwaji, 2008). The MDI magnetogram images show the footprint of the magnetic fields of the solar photosphere, with dark and light areas indicating opposite magnetic polarities. These dark and light areas are detected separately and combined afterwards to determine the active region candidates.

- Apply region growing to combine sunspot and active region candidates. In the region growing technique small areas of candidate pixels are iteratively merged according to similarity constraints. This technique is described in (Colak and Qahwaji, 2008).
- Use neural networks to combine regions of opposite magnetic polarities in order to determine the exact boundaries of sunspot groups.
- Mark the detected sunspot groups.

McIntosh-based classification

- Extract local features from every sunspot in every group using image processing and neural networks.
    - Extract the length, height and area of the sunspot.
    - Use neural networks to determine the type of penumbra (i.e., Mature or Rudimentary) and whether the sunspot is Symmetric or Asymmetric.
- Extract features from each sunspot group using image processing. The extracted features are length, largest spot, polarity and distribution.
- Apply all the extracted features to a decision tree to determine their McIntosh classification.

3 Solar Flare Prediction using Machine Learning

Solar flare research has shown that flares are closely related to sunspots and active regions. A survey of the solar physics literature describing the association between flares and sunspots was presented in (Qahwaji and Colak, 2007).

The system we introduce here extracts the information embedded in historical data (i.e., solar catalogues) and represents it in computerized learning rules that enable computers to analyze current solar data and provide objective predictions. The implementation of this system is discussed below.

3.1 Knowledge Representation of Historical Data

Data from the publicly available sunspot group catalogue and the solar flare catalogue provided by the National Geophysical Data Centre (NGDC) are compared to find the associations between sunspots and flares. NGDC keeps records of data from several observatories around the world and holds one of the most comprehensive publicly available databases for solar features and activity. The NGDC flare catalogue provides information about dates, starting and ending times for flare eruptions, location, x-ray classification, and the National Oceanic and Atmospheric Administration (NOAA) number for the active regions that are associated with the detected flares, while the NGDC sunspot catalogue provides information about the date, time, location, physical properties, and classification of sunspot groups. This sunspot catalogue has sunspot data from different observatories around the world and sometimes includes several observations of the same sunspot group for different times of day.

Both catalogues are investigated to associate solar flares with the sunspot groups that have caused them. All the reported flares and sunspots for the periods from 1st January 1982

till 31st December 2006, which includes 36736 solar flares (32151 C-class, 4258 M-class and 337 X-class) and 186324 sunspot groups, are analyzed using the association algorithm described in (Qahwaji and Colak, 2007). The association algorithm is based on comparing the NOAA number and occurrence time of sunspot groups and solar flares. The algorithm would associate a sunspot group and a solar flare, only if their NOAA numbers are same and if solar flare is observed within 24 hours after the sunspot group is observed. Before applying the algorithm, these catalogues are first analyzed using a computer program to check if the recorded sunspot groups have NOAA numbers, location information, and classification information. In some cases, some of the sunspot groups in the NGDC catalogue have invalid McIntosh classifications, as shown in Table 1. We have modified our computer program to verify if the reported sunspot group classifications on the NGDC sunspot catalogue are valid McIntosh classifications. After eliminating the sunspot groups that have missing or wrong entries in the sunspot catalogue, as shown in Table 1, the available number of sunspot groups has been reduced to 166719. It was also found that only 21713 solar flares (18136 C-class, 3272 M,-class, and 305 X-class) out of 36736 flares have NOAA numbers in the NGDC solar flare catalogue.

Table 1: Some examples of wrong McIntosh classes and/or missing data in the NGDC catalogue for the first months of 1982.

11820101	1249	S19W73	B	3532	CXO	4	4	130	811227.0	811227.3	517	3RAMY
11820114	0125	N03E26	B	3550	BXX	2	3		820116.0	820115.9	22	3LEAR
11820117	0055	S08W26	B	3553	HSO	8	7	20	820115.1	820115.0	25	4LEAR
11820118	1600	N09E30	A	3552	FSX	1	1	50	820120.9	820121.0	402	3BOUL
11820118	1600	S11W27	BG	3549	DS	10	7	200	820116.6	820117.0	399	3BOUL
11820118	1600	S14W13	B	3559	DA	8	7	280	820117.7	820117.7	405	3BOUL
11820127	1605	N09E47	B	3573	CKX	9	9	350	820131.2	820201.0	418	3BOUL
11820210	1931	S08E06	BD	3603	CKC	32	10	450	820211.3	820211.3	71	3HOLL
11820215	1500	N13E70	B	3610	C O	3	6	20	820220.9	820221.1	79	2HOLL
11820217	1555	N06E19	A	3612B	RX	1		10	820219.1	820219.2	455	3BOUL
11820304	1400	N13W37	B	3625	DK	7	6	610	820301.8	820302.0	82	3RAMY

The association algorithm has managed to associate a total of 37515 sunspot groups with solar flares using their NOAA numbers and the 24 hours time difference. These 37515 sunspot groups are associated with 72727 C-class solar flares, 12103 M-class solar flares, and 1081 X-class solar flares. The difference between the total number of solar flares and the number of associated sunspots is caused by the fact that a sunspot group could produce more than one solar flare within the 24 hours time period. Also, there are multiple observations (3 to 4 observations per day) of the sunspot groups that are included in the NGDC sunspots catalogue. Hence, a solar flare can be associated with the same sunspot group that is reported more than once within 24 hours.

3.2 The Flare Prediction system

The learning system introduced in this work is inspired by our previous work in (Qahwaji and Colak, 2007). Learning algorithms such as Neural Network (NN), Support Vector Machines (SVM) and Radial Bases Functions (RBF) were optimized, trained and then compared for flare predictions in (Qahwaji and Colak, 2007). In this work, features such as McIntosh classifications and daily sunspot numbers were used as inputs to the learning algorithms. The training and generalization performances of the learning algorithms were evaluated using testing tools such as the Jack-knife technique (Fukunaga, 1990). In this paper we are using the area of sunspot groups together with the McIntosh classes as inputs to the learning algorithms in order to generate predictions for the C-class, M-class and X-class flares.

Our solar flare prediction algorithm is composed of two Neural Network (NN) systems that are working together as illustrated in Figure 2. The first NN uses the numerical representations of the three parts of the McIntosh classification for the sunspot region under

consideration together with its sunspot area as inputs. It generates the probability that this sunspot region will produce a C-class, M-class or X-class solar flare in the next 24 hours. Hence, this NN has four input nodes and one output node and is trained using sunspot regions and solar flare associations as described in the previous section. The training vector for this NN contains numerical values representing the four inputs and their corresponding target as shown in Table 2. The target represents the actual "FLARE" / "NO FLARE" cases. For example, if there is a sunspot region with a McIntosh classification of FKI and an area of 600 in millionths of solar hemisphere that is associated with a C-class, M-class or X-class flare then the training vector will be [0.9, 0.9, 0.5, 0.24; ***0.9***].

Table 2: Inputs and output values for first neural network used for determining the flaring probability.

Inputs				Output
McIntosh classes				
A= 0.10 H= 0.15 B= 0.30 C= 0.45 D= 0.60 E= 0.75 F= 0.90	X= 0 R=0.10 S=0.30 A=0.50 H=0.70 K=0.90	X=0 O=0.10 I=0.50 C=0.90	Normalized (with 2500) sunspot area	FLARE =0.9 NO FLARE= 0.1

When the first NN predicts that a flare is going to occur, the second NN is activated to determine whether the predicted flare is going to be C-class, M-class and/or X-class flare. The second NN is trained using a new training set that contains only the sunspot groups that were associated with C-class, M-class and X-class flares. Hence, the second NN consists of four inputs and three outputs. The first, second and third outputs represent the C-class, M-class and X-class flares, respectively. These outputs are assigned as described below:

If the sunspot group is associated only with a C-class flare, then the first output will be 0.9 otherwise it will be 0.1.

If the sunspot group is associated only with a M-class flare, then the second output will be 0.9 otherwise 0.1.

If the sunspot group is associated only with a X-class flare, then the third output will be 0.9 otherwise 0.1.

If the sunspot group is associated with more than one type of solar flare, all the corresponding outputs (first output for C-class, second output for M-class, and third output for X-class) will be 0.9 otherwise 0.1.

For example, if there is a sunspot region with a McIntosh classification of EKI and an area of 500 in millionths of solar hemisphere that is associated only with C-class and M-class solar flares at the same time then the training vector will be [0.75, 0.9, 0.5, 0.20; ***0.9, 0.9,0.1***].

3.3 Optimization of the Neutral Networks Prediction System

The two neural networks are optimized by finding the minimum Mean Squared Error (MSE) during training for different NN topologies. MSE is calculated using Equation (1):

$$\mathrm{MSE} = \frac{1}{n}\sum_{i=1}^{n}(p_i - r_i)^2 \tag{1}$$

Where, n is the total number of examples in the training vector, p_i is the calculated value of each output for the inputs given in the training vector, and r_i is the real output value given in the training vector.

Several training experiments are carried out while changing the number of nodes in the hidden layer from 1 to 20. For every new experiment the MSE of the training is recorded and the number of hidden nodes with the least MSE is chosen. Both networks are optimized by using one hidden layer with ten nodes for the first NN and twelve nodes for the second NN.

4 Practical Implementation and Evaluation of the Hybrid System

The imaging and machine learning systems are integrated for the hybrid solar flare prediction system. The final system is shown in Figure 3. The complete integrated hybrid system provides automated prediction of solar flares from MDI images. The system starts its real-time operations by processing SOHO/MDI continuum and magnetogram images in the manner explained in Section 2 to provide automated McIntosh classifications for the detected sunspots. Then the McIntosh classified sunspots and their calculated areas are fed to the machine learning system described in Section 3 which is trained with 14 years of data after applying the association algorithm. Based on the embedded learning rules the system predicts if a solar flare is going to occur or not. If a major solar flare is predicted then the probability of this solar flare to be C-class, M-class or X-class flare is also predicted. The entire system is implemented in C++. It takes about 15 seconds to process the latest SOHO/MDI continuum and magnetogram images and generate these predictions. A working version of this system is currently available at http://spaceweather.inf.brad.ac.uk/. This version is real-time, fully automated and web-compliant.

4.1 Evaluation of the System

The performance of the hybrid system was evaluated by comparing the generated predictions with the actual flares as reported by NOAA SWPC[1] in the NGDC X-ray solar flare catalogue. The system was tested on solar MDI intensitygram images from February 1, 1999 to December 31, 2002. This period included intervals of high solar activity that produced a considerable number of C-class, M-class and X-class solar flares and investigating periods of high-activity is important for the effective evaluation of our system.

[1] http://www.swpc.noaa.gov/

There were 5267 MDI continuum (intensitygram) images available during this period at a cadence of four images per day. These MDI continuum images and their corresponding 5267 MDI magnetogram images were processed using the hybrid system and a sunspot catalogue was created which we refer to as the Automated Sunspot Catalogue (ASC). Parts of the ASC are shown in Table 3. All the automatically detected and classified sunspot groups, which are taken for April 1, 2001 at 00:00 and at 06:24, along with their flaring probabilities are provided. It is known that smaller flares occur more frequently than larger flares. However, our hybrid system could generate higher X-class flare probability compared to M-class probability for some sunspot groups. An example for this can be seen for the FKC sunspot group detected on N17W36 at 00:00 and on N17W40 at 06:24. These probabilities are generated by NNs which are trained with years of historical data representing sunspot groups and their associated solar flares. After convergence in training is reached, the NN accepts new set of inputs and generates outputs based on the learning rules and weights formed during training. From these outputs it can be understood that most of the groups with FKC classification and with an area of around 1500 square degrees are more likely to produce a X-class flare than M-class flare when the historical associations are considered. In addition to the ASC, the hybrid system displays its predictions on a web page as shown in Figure 4. The generated images show the detected sunspot groups and their flaring probabilities.

In order to test the hybrid system we compared the solar flare predictions of each sunspot group in ASC to the x-ray solar flares reported in the NGDC solar flare catalogues. Between February 1, 1999 and December 31, 2002 there were 5175 reported C-class, M-class and X-class solar flares with location information. Out of these 5175 solar flares 4469 of them were C-class, 663 of them were M-class and 43 of them were X- class flares.

Table 3: The Automated Sunspot Catalogue (ASC). L (Length of the sunspot group), N (Number of sunspots within the group), F (Flaring Probability), C (Probability of the flare to be C class), M (Probability of the flare to be M class), X (Probability of the flare to be X class).

Date	Time	Loc.	Class	N.	L.	Area	F.	C.	M.	X.
01/04/01	00:00	N25E28	HKX	1	4	132	0.158	0.136	0.121	0.079
01/04/01	00:00	N17W36	FKC	43	37	1440	0.746	0.635	0.203	0.322
01/04/01	00:00	N11E27	CSO	6	9	79	0.084	0.076	0.064	0.019
01/04/01	00:00	N08W04	HRX	1	1	1	0.113	0.102	0.030	0.014
01/04/01	00:00	S05E08	DSO	18	6	74	0.099	0.091	0.073	0.013
01/04/01	00:00	S10W16	FKC	35	35	450	0.648	0.578	0.516	0.269
01/04/01	00:00	S11W72	BXO	6	8	49	0.108	0.095	0.076	0.053
01/04/01	00:00	S13E64	AXX	1	1	153	0.103	0.092	0.014	0.000
01/04/01	00:00	S24E23	BXO	2	1	3	0.108	0.095	0.082	0.055
01/04/01	00:00	S36E30	AXX	1	1	4	0.116	0.103	0.027	0.016
01/04/01	06:24	N25E25	HKX	1	4	134	0.158	0.136	0.121	0.079
01/04/01	06:24	N17W40	FKC	41	37	1558	0.750	0.624	0.036	0.204
01/04/01	06:24	N11E24	CSO	5	9	65	0.080	0.073	0.062	0.019
01/04/01	06:24	N10W07	CAO	3	3	28	0.078	0.070	0.058	0.039
01/04/01	06:24	S01W30	BXO	2	1	9	0.108	0.095	0.082	0.054
01/04/01	06:24	S05E04	DSO	17	6	128	0.119	0.109	0.091	0.017
01/04/01	06:24	S09W19	FKO	29	35	533	0.593	0.509	0.543	0.291
01/04/01	06:24	S12W75	BXO	2	6	68	0.108	0.095	0.073	0.052
01/04/01	06:24	S13E60	AXX	1	1	151	0.103	0.092	0.014	0.000

In order to associate the sunspot groups detected by our algorithms with x-ray solar flares reported in the NGDC catalogue, we had to modify the association algorithm, introduced in (Qahwaji and Colak, 2007), to compare sunspots and solar flares based on their locations (latitude and longitude) not their NOAA numbers. The new modifications are necessary because the sunspot groups in ASC do not have NOAA numbers. Also, not all the solar flares reported in NGDC flare catalogue have location information and these solar flares are not included in this study. The association algorithm that we have used here is explained below:

- Read all the sunspot groups and their solar flare predictions as reported in ASC.

- Read the actual M and X-class flares with location information as reported in the NGDC solar flare catalogue.
- Carry out extensive search to associate each actual flare with its corresponding sunspot group by comparing their longitude, latitude, and time information. In order to confirm that a sunspot group and a solar flare are associated the following criteria must be met:
    - The difference in time between the detected sunspot group and its associated flare must be less than 6, 12, 24, 48, and 72 hours, depending on the forecast lead time objective.
    - Sunspot group locations must be corrected for solar rotation (The new coordinates are calculated using Carrington Heliographic coordinates) depending on the time difference between sunspot group and solar flare under consideration
    - The solar flare must be within the 10 degree radius of corrected sunspot location.
- If all the criteria are satisfied then this sunspot group is highlighted as being associated with a solar flare, otherwise it is considered not to be associated.

After the completion of the association process the prediction performance is evaluated using various verification measures as explained below.

4.2 Verification Results

The hybrid system generates predictions in numerical format, between 0.0 and 1.0, as shown in Table 3. In order to evaluate the predictions of the hybrid system several measures are used. Some of these measures require forecast probabilities and some of them require categorical forecasts (Yes/No) as inputs for assessing the outputs of the hybrid system. For the measures that require forecast probabilities the outputs of the hybrid system are used by directly converting them to percentages. For example, if the flaring output of the system is

0.23, it is assumed that the sunspot group under consideration has a 23% flaring probability. As for categorical forecasts (Yes/No); a threshold value of 0.5 (50%) is used for determining the final predictions. Our training data includes output values 0.1 (10%) and 0.9 (90%) for non-flaring and flaring sunspot groups respectively and therefore if the output generated by the hybrid system is above this threshold value then it is assumed that a flare is predicted to occur. On the other hand, if the generated output is less than the threshold value then no flare is expected.

In order to calculate the success of the generated predictions the association results are investigated using the following four criteria:

- If a sunspot group is associated with an actual flare, as explained previously, and a flare prediction is generated then this prediction is successful.
- If a sunspot group is associated with an actual flare but no flare prediction is generated then this prediction is not successful.
- If a sunspot group is not associated with any actual flare and no flare prediction is generated then this prediction is successful.
- If a sunspot group is not associated with any actual flare but a flare prediction is generated then this prediction is not successful.

The solar flares with location information during the verification period (February 1, 1999 to December 31, 2002) are compared with 40534 sunspot groups that were detected from 5267 MDI image pairs and recorded in ASC.

The prediction results are compared for different time windows: 6, 12, 24, 48 and 72 hours. Several forecast verification measures are used to evaluate our results for each time window as shown in Table 4. The measures used are: Probability of Detection (POD), False

Alarm Rate (FAR), Percent Correct (PC), Heidke Skill Score (HSS) and Quadratic Score (QR). These forecast measures are defined well in a recent paper by (Balch, 2008) and readers can refer to this paper for more information.

Table 4: Prediction evaluation measures for 6, 12, 24, 48, and 72 hours. The measures used are: Probability of Detection (POD), False Alarm Rate (FAR), Percent Correct (PC), Heidke Skill Score (HSS) and Quadratic Score (QR). The HOURS column show the different time windows while the CLASS column represents the different individual solar flare classes (C, M, and X) except for F which represents the evaluation for all solar flare classes.

HOURS	CLASS	QR	POD	FAR	PC	HSS
6	ALL	0.083	0.432	0.655	0.890	0.382
	C	0.074	0.363	0.680	0.904	0.378
	M	0.035	0.413	0.894	0.965	0.250
	X	0.021	0.278	0.992	0.983	0.033
12	ALL	0.107	0.703	0.478	0.857	0.494
	C	0.100	0.644	0.506	0.867	0.479
	M	0.040	0.732	0.801	0.957	0.398
	X	0.022	0.667	0.982	0.982	0.096
24	ALL	0.146	0.814	0.301	0.805	0.512
	C	0.141	0.772	0.319	0.811	0.493
	M	0.050	0.865	0.688	0.944	0.470
	X	0.022	0.917	0.967	0.981	0.169
48	ALL	0.196	0.860	0.166	0.737	0.494
	C	0.194	0.829	0.171	0.737	0.474
	M	0.065	0.916	0.558	0.922	0.503
	X	0.023	0.957	0.932	0.979	0.262
72	ALL	0.228	0.875	0.123	0.694	0.475
	C	0.228	0.848	0.117	0.692	0.457
	M	0.075	0.929	0.481	0.908	0.510
	X	0.024	0.968	0.908	0.978	0.310

The quadratic score (QR) is simply the mean square error of the probabilities provided by the hybrid system. QR is used to calculate the accuracy in probability predictions. A

smaller QR indicates better accuracy in predictions. A perfect QR which is of zero value would require an accurate prediction of solar flare every time a solar flare occurs and an accurate prediction of no activity when no flares occur (Balch, 2008). Best QR results are achieved for 6 hours time window and QR increases slightly while the time window is extending. We also used QR to compare our results with the 1, 2, and 3 days prediction results from NOAA Space Weather Prediction Center (SWPC) for the same dates, as shown in Table 5. The average QR (or mean square error) between 1999 and 2002 are also calculated and show in this Table. When we compare these average results with the results from ASAP for the same dates, it can be seen that ASAP provides better accuracy in predictions than SWPC especially for M-class flare predictions. Also X-class flare predictions of ASAP are better than SWPC in average although SWPC achieved the least QR for X-class flare prediction during 1999.

Table 5: Comparison of QR measures for 24, 48, and 72 hour time windows from ASAP and Space Weather Prediction Center (SWPC). SWPC results can be accessed from their website[2].

	DATE	CLASS	24	48	72
ASAP	1999-2002	M	0.050	0.065	0.075
		X	0.022	0.023	0.024
SWPC	1999	M	0.178	0.190	0.192
		X	0.017	0.019	0.018
	2000	M	0.210	0.223	0.228
		X	0.039	0.040	0.042
	2001	M	0.190	0.198	0.201
		X	0.050	0.048	0.047
	2002	M	0.226	0.229	0.240
		X	0.033	0.033	0.033
	Average	M	0.210	0.210	0.215
		X	0.034	0.035	0.035

[2] http://www.swpc.noaa.gov/forecast_verification/ Last Access:2008

POD measures the probability of actual solar flares being predicted correctly by the hybrid system. Best POD results are achieved for the 72 hour time window. It is expected that POD would increase with time since there are more solar flare occurrences in larger time windows. For 24 hours time difference POD results show that 81.4% of the whole reported solar flares (77.2% of the C-class flares, 86.5% of the M-class flares and 91.7% of the X-class flares) are predicted correctly. FAR measures the probability of the hybrid system predicting a solar flare that actually does not occur. Although FAR decreases when the time window extends for all kind of flares, it is still very high for X-class predictions and false alarm rate has to be decreased in order to increase the reliability of the system.

PC measures the correct prediction rate of the overall system which is the ratio of successful flare and no flare predictions generated by our hybrid system. PC rates show that for 24 hours time difference, 80.5% of all the predictions (flare or no flare), 81.1% of C-class predictions (C-class or not a C-class), 94.4% of M-class predictions (M-class or not a M-class), and 98.1% of X-class predictions (X-class or not a X-class) are correct. Although PC rates are very high, it must be noted that if the system provides just one output, which is no-flare, these rates would still be high.

HSS is a measure showing the chance factor in predictions. HSS can range from -1 (for no correct predictions) to +1 (for all correct predictions) and a value of zero indicates that the predictions have been generated mainly by chance. This is a very useful measure for the verification of the systems especially when occurrences of the events to be predicted are very rare. As mentioned above, even if our systems outputs would have been set to be no-flare all the time, our predictions would be correct by more than 90%. Therefore, HSS is a very important measure for evaluating our prediction performance. HSS results show that ASAP

predictions are much more than chance especially for flaring and C- and M-class flare predictions. HSS can also be used to optimize the system by changing the threshold value (0.5 was used for our calculations as described earlier) and achieve better prediction results.

To provide further evaluation for the system we created a forecast reliability diagram. The reliability diagram plots the observed frequency against the forecast probability, where the range of forecast probabilities is divided into bins. Figure 5 plots the observed frequency of all the flaring sunspot groups against their corresponding prediction probabilities, grouped in 5% (0.05) bins (0%-5%(0-0.05), 5%-10%(0.05-0.1), 10%-15%(0.1-0.15), …). The dashed diagonal line represents perfect correspondence. This reliability chart is produced by comparing the predictions of ASAP for 24 hours time window and includes the output from the main Neural network of the system that decides if the sunspot group is going to produce a flare or not. The reliability diagram is similar to a scattered plot, where the sunspot groups are stratified by their flaring forecast into probability bins and the observed flaring frequency of these sunspot groups are calculated. For example, if there are 10 sunspot groups with calculated flaring probabilities that varies between 5% and 10%, and in reality 3 (30%) of them produced flares, then this means that the calculated flaring probabilities are lower than it should be and it is not a very reliable system. As it can be seen from Figure 5, our results are showing good correspondence and are highly reliable. Also this diagram shows that there are no flare prediction probabilities produced by our system that are higher than 80% and therefore the forecast bins after 75%-80% bin are empty.

5 Conclusions

In this paper we have introduced, for the first time, a fully automated hybrid system called ASAP that integrates advanced machine learning and image processing techniques with

solar physics to predict automatically whether a sunspot group is going to produce a solar flare and whether the predicted flare is going to be a C-class, M-class or X-class flare.

The performance of the hybrid system depends on the generalization capabilities of the machine learning system and the grouping and classification performance of the image processing system. For our hybrid system the HSS, POD, PC, and QR measures are quite good particularly when predicting that a solar flare is going to erupt. Especially HSS is very promising which shows that ASAP predictions are much better than chance. However, the same thing cannot be said for the FAR measure. This is a problem that has to be tackled especially for X-class flare predictions which we are planning to solve in the near future. Also comparison of QR results of ASAP and SWPC showed that ASAP provides better prediction results than SWPC especially for M-class flares.

The prediction rates for the hybrid systems can be improved by exploiting the generalization capability of machine learning system. Better generalization is obtained when more training data are used. Hence, we believe that it is important to monitor the performance of the hybrid system during its initial stages which includes comparing the prediction performance with the actual flares reported by NOAA. Evolutionary algorithms may be used to allow the learning algorithms to evolve and provide better optimization and generalization.

The geometric effect on MDI images close to the limb also affects the classification of sunspot groups which would lead to wrong prediction results. Although, most of the calculations needed for classification are carried out in heliographic coordinates, the lack of graphical information towards the limb is the main problem preventing us from obtaining more-accurate classifications. For example, large sunspot groups just starting to appear from the limb are more likely to be classified incorrectly (Colak and Qahwaji, 2008).

An automated and real-time version of ASAP is running on our website at http://spaceweather.inf.brad.ac.uk/index.html since March 2007. This system connects automatically to SOHO's website[3] to download the latest MDI continuum and magnetogram images. After automatically running the algorithms described in this paper the results are displayed on our website as shown in Figure 4 and are updated automatically. ASAP is available publicly for download at http://spaceweather.inf.brad.ac.uk/downloads.html.

The processing time for our system is approximately 15 seconds to process the two MDI images and to generate the predictions on an Intel Centrino machine with 2 Gb memory. This enables our system to provide near-real time classifications and predictions. The system can be modified to accept other types of solar images. Sometimes the characteristics of a sunspot group can change rapidly in hours and cause flares, it is almost impossible for a human observer to determine what triggers this process without having the appropriate tools. We believe that the system introduced here can help researchers or observers investigate and understand solar features and activity and identify patterns that could be useful for space weather predictions.

In our previous work (Qahwaji et al., 2007), (Qahwaji and Colak, 2007), we have shown that SVM provides better generalization performance compared to NN. In the near future we will integrate these findings and use SVM networks to enhance the predictions. We also believe designing a sunspot group tracking system that studies the evolution of the sunspot groups can improve the overall performance. Moreover, we believe that we need to take into consideration the magnetic properties and energies of the sunspot regions under investigation. Very recently, we designed an algorithm (Ahmed et al., 2008) that would analyze magnetogram images to estimate the magnetic energy of an active region based on the Ising

[3] http://sohowww.nascom.nasa.gov/data/realtime/ Last Access: 2008

model. In the future we are planning to implement this magnetic energy parameter to the flare prediction part of the system to improve the reliability of the predictions.

Acknowledgements

This work is supported by EPSRC (GR/T17588/01) and (EP/F022948/1) grants, which are entitled “Image Processing and Machine Learning Techniques for Short-Term Prediction of Solar Activity” and "Image Processing, Machine Learning and Geometric Modeling for the 3D Representation of Solar Features", respectively.

References

AHMED, O., QAHWAJI, R., COLAK, T., WIT, T. D. D. & IPSON, S. (2008): A New Method for Processing Solar Images to Calculate the Magnetic Energies Associated with Active Regions., Accepted for publication in IEEE Fifth International Multi-conference on Systems, Signals, and Devices - International Conference on Systems Analysis and Automatic Control.

BALCH, C. C. (2008): Updated verification of the Space Weather Prediction Center's solar energetic particle prediction model. Space Weather 6,

COLAK, T. & QAHWAJI, R. (2008): Automated McIntosh-based classification of sunspot groups using MDI images. Solar Physics, 248/ 2, 277-296

FUKUNAGA, K. (1990): Introduction to Statistical Pattern Recognition. Academic Press, New York.

GALLAGHER, P. T., MOON, Y. J. & WANG, H. M. (2002): Active-region monitoring and flare forecasting - I. Data processing and first results. Solar Physics 209/1, 171-183.

KOSKINEN, H., TANSKANEN, E., PIRJOLA, R., PULKKINEN, A., DYER, C., RODGERS, D. & CANNON, P. (2001): Space Weather Effects Catalogue. ESA Space Weather Programme Feasibility Studies FMI, QinetiQ, RAL Consortium.

LENZ, D. (2004): Understanding and Predicting Space Weather. The Industrial Physicist 9/6, 18-21.

MCINTOSH, P. S. (1990): The Classification Of Sunspot Groups. Solar Physics 125/2, 251-267.

MEEUS, J. (1998): Astronomical Algorithms - Second Edition. Willmann-Bell, Inc., Virginia.

MILLER, R. W. (1988): Wolf - A Computer Expert System For Sunspot Classification And Solar-Flare Prediction. Journal Of The Royal Astronomical Society Of Canada 82/4, 191-203.

PICK, M., LATHUILLERE, C. & LILENSTEN, J. (2001): Ground Based Measurements.. ESA Space Weather Programme Feasibility Studies Alcatel-LPCE Consortium.

QAHWAJI, R. & COLAK, T. (2007): Automatic Short-Term Solar Flare Prediction Using Machine Learning and Sunspot Associations. Solar Physics 241/1, 195-211.

QAHWAJI, R., COLAK, T., AL-OMARI, M. & IPSON, S. (2007): Automated Machine Learning Based Prediction of CMEs Based on Flare Associations Topical Issues in Solar Physics,

SCHERRER, P. H., BOGART, R. S., BUSH, R. I., HOEKSEMA, J. T., KOSOVICHEV, A. G., SCHOU, J., ROSENBERG, W., SPRINGER, L., TARBELL, T. D., TITLE, A., WOLFSON, C. J., ZAYER, I., AKIN, D., CARVALHO, B., CHEVALIER, R., DUNCAN, D., EDWARDS, C., KATZ, N., LEVAY, M., LINDGREN, R., MATHUR, D., MORRISON, S., POPE, T., REHSE, R. & TORGERSON, D. (1995): The solar oscillations investigation - Michelson Doppler Imager. Solar Physics 162/1-2, 129-188.

WANG, H., QU, M., SHIH, F., DENKER, C., GERBESSIOTIS, A., LOFDAHL, M., REES, D. & KELLER, C. (2003): Innovative Information Technology for Space Weather Research. AAS 204th Meeting, Session 52 Virtual Observations in Solar Physics. The American Astronomical Society.

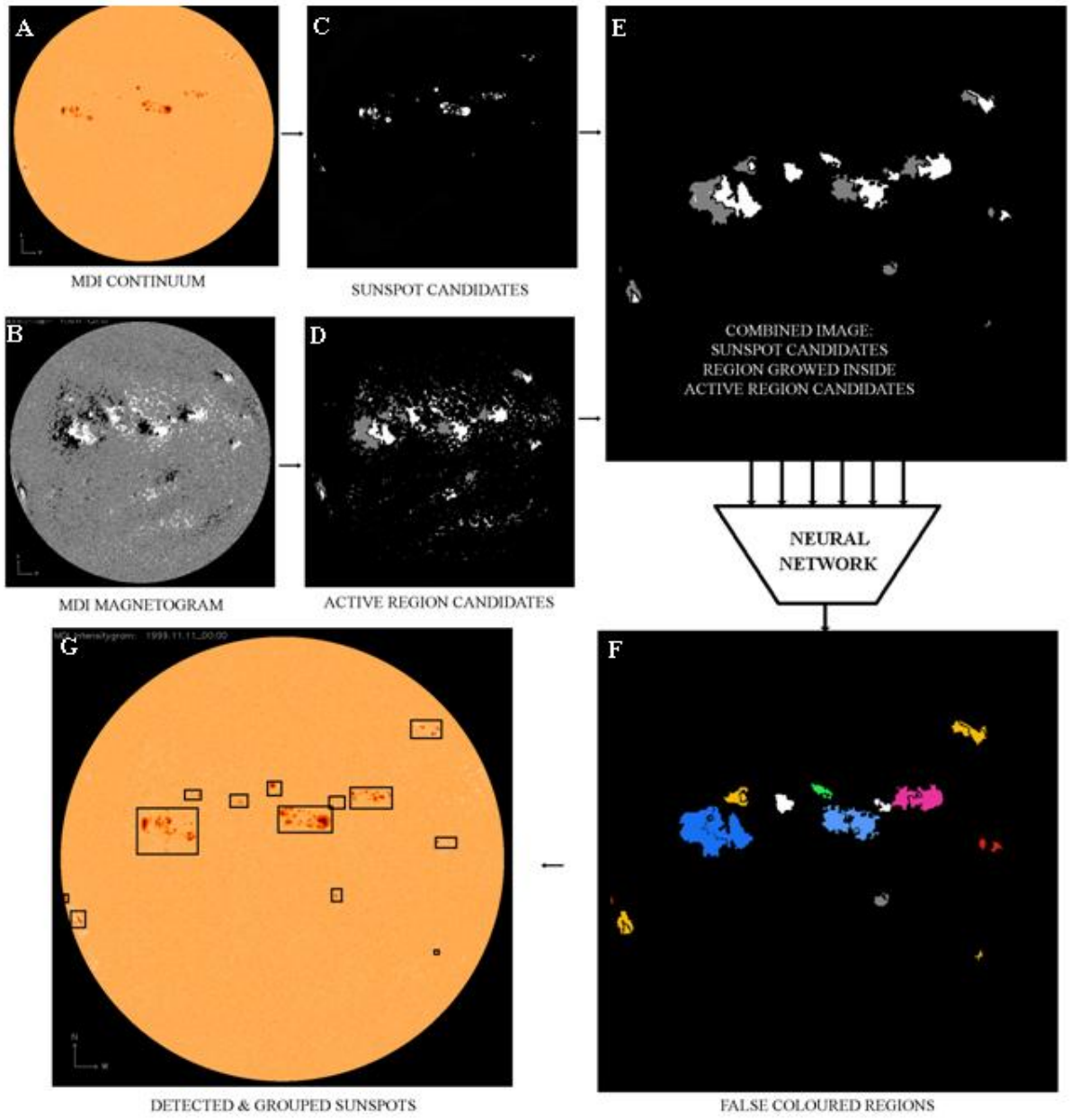

Figure 1: The Stages and results of sunspot detection and grouping process. Image A and B are the continuum and magnetogram images respectively. Image C shows the detected sunspots, image D shows detected active regions. These images are combined using region growing in image E to show the exact locations of active regions. Using Neural Networks active regions are classified into groups in image F and this data is also used to detect sunspot groups in image G.

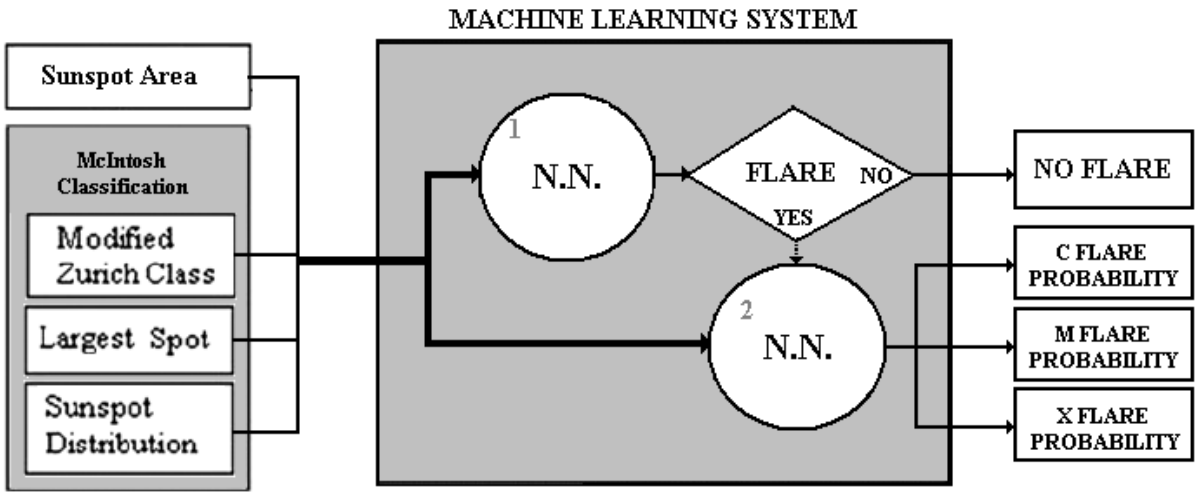

Figure 2: Machine learning system for flare prediction.

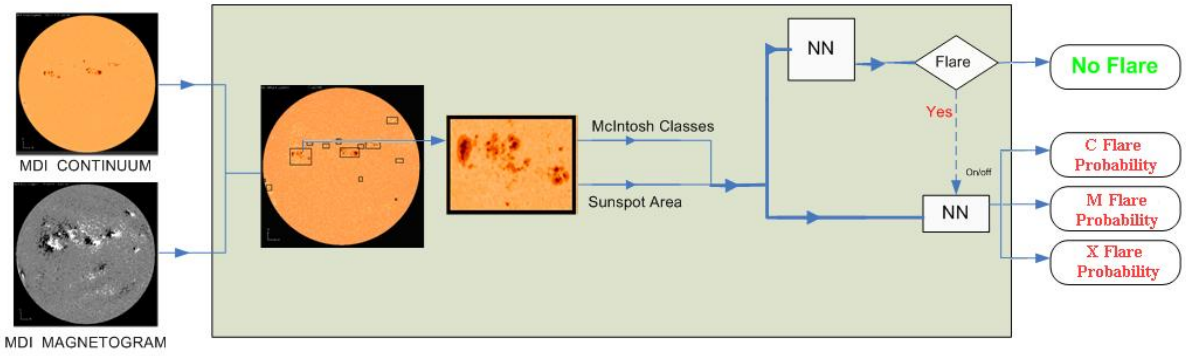

Figure 3: The final hybrid system

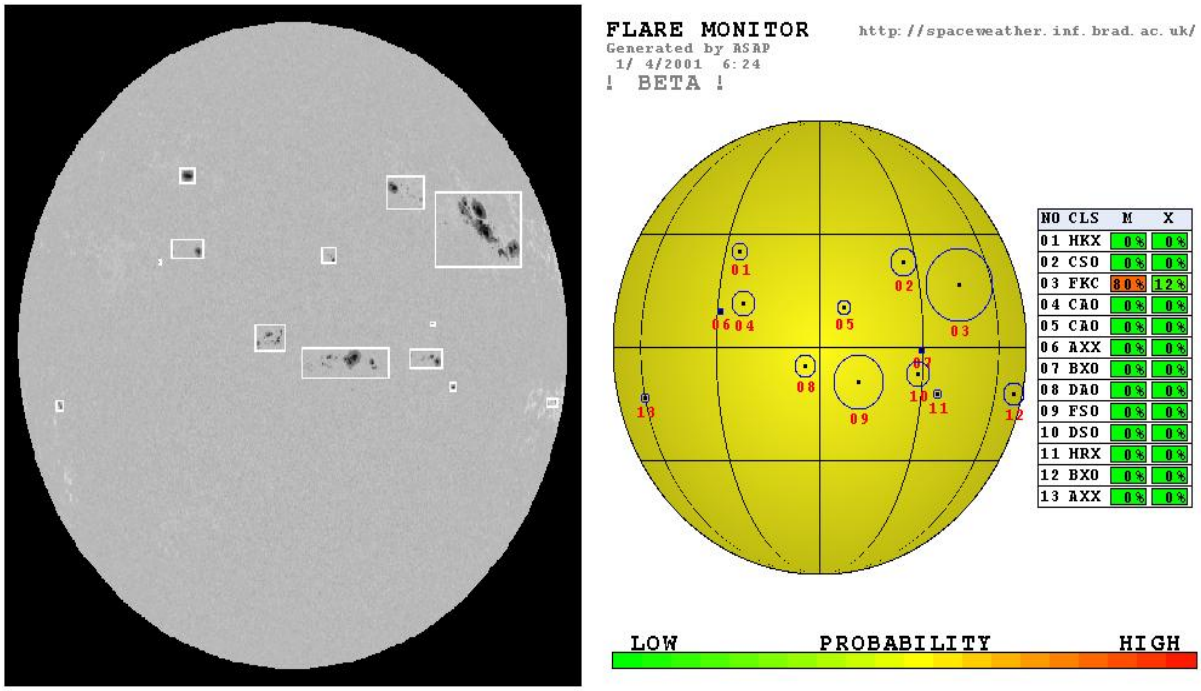

Figure 4: Two images generated by the hybrid system. The image to the left shows the detected sunspot groups and the image to the right shows the classification and flare probabilities of the detected sunspot groups. The image to the right is updated automatically on http://spaceweather.inf.brad.ac.uk/index.html every time a new MDI continuum image is available on SOHO's website.

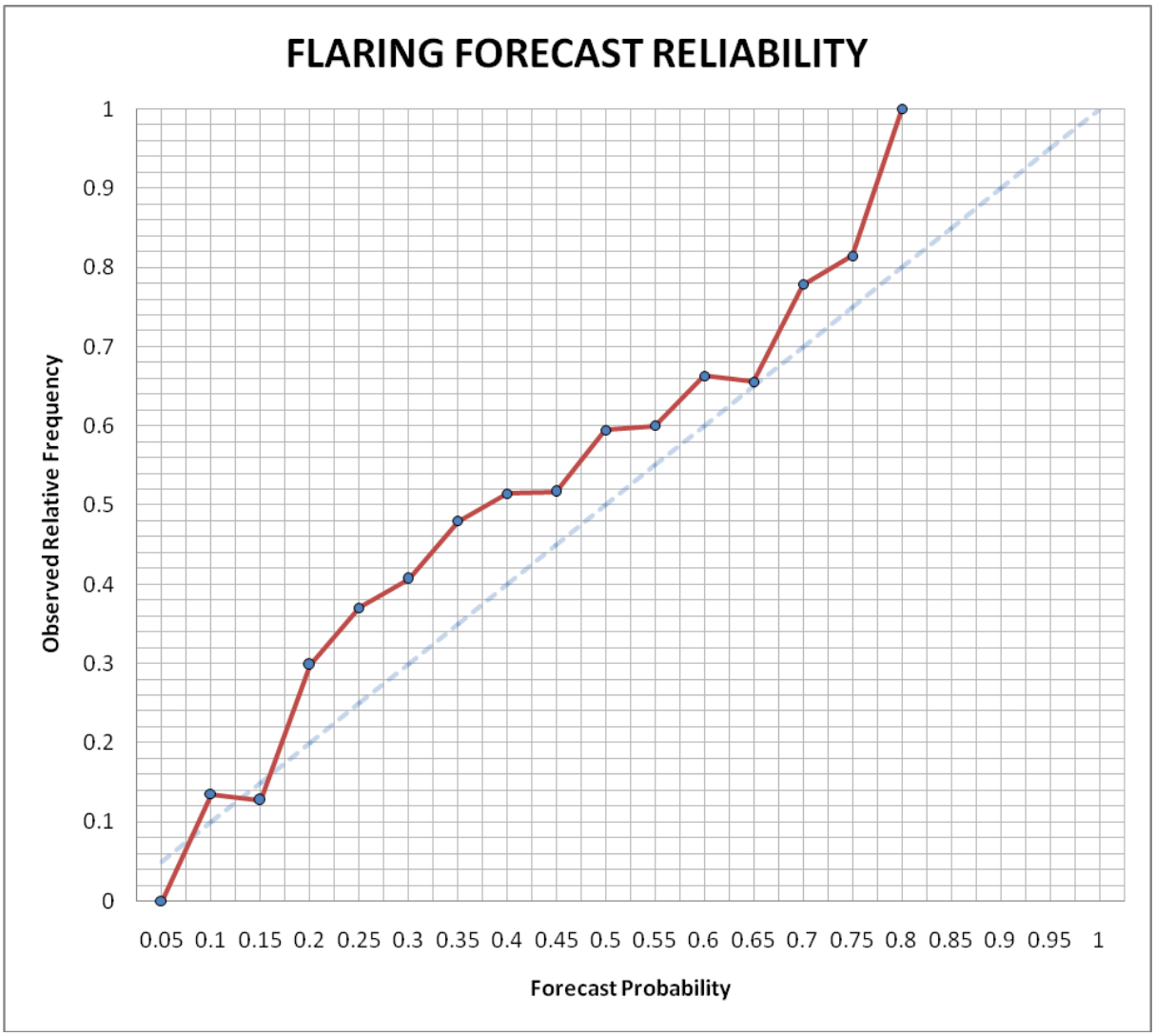

Figure 5: The observed relative frequency of all the flaring sunspot groups against their corresponding predictions, grouped in 5% (0.05) bins.